Extended Abstracts of the 2018 International Conference on Solid State Devices and Materials, Tokyo, 2018, pp703-704

Manipulated Circular Polarized Emission of Tungsten Diselenide (WSe_2) Atomic Layers with Chiral Plasmonic Metasurface

Hsiang-Ting Lin[1,2], Chiao-Yun Chang[1], Pi-Ju Cheng[1], Ming-Yang Li[1,3], Chia-Chin Cheng[3], Shu-Wei Chang[1,2], Lain-Jong Li,[3] Chih-Wei Chu[1], Pei-Kuen Wei[1], and Min-Hsiung Shih[1,2,4*]

[1] Academia Sinica
Research Center of Applied Sciences (RCAS)
Taipei, 11529, Taiwan
Phone: +886-2-2787-3184 E-mail: mhshih@gate.sinica.edu.tw
[2] National Chiao Tung University
Department of Photonics & Institute of Electro-Optical Engineering
Hsinchu 30010, Taiwan
[3] King Abdullah University of Science and Technology (KAUST)
Physical Science and Engineering Division
Jeddah 23955-6900, Kingdom of Saudi Arabia
[4] National Sun Yat-sen University
Department of Photonics
Kaohsiung 804, Taiwan

Abstract

An ultrathin and circularly polarized controllable light source were demonstrated by integrating the WSe_2 atomic layers with plasmonic chiral metasurfaces. The intrinsic chiral emission of WSe_2 was manipulated by chiral metasurfaces to achieve a 400% emission circular dichroism enhancement than bare WSe_2.

1. Introduction

Controlling circularly polarized (CP) states of light can be applied on various areas from bio-sensing to optical communication. [1] Recently, the attractive transition metal dichalcogenides (TMDCs) atomic layers have been demonstrated to exhibit unusual CP emission, which are the results of selective CP state absorption in the K-valley of TMDCs lattices. [2] The promising TMDCs atomic layers could be integrated with chiral plasmonic metasurfaces to achieve CP emission manipulation. The confinement of localized surface plasmon resonance (LSPR) modes in chiral metasurfaces could generate strong local optical chirality [3] when integrated with low dimensional materials such as TMDCs atomic layers. In this study, we investigated a nanorod based chiral metasurfaces to manipulate the CP emission of monolayer TMDC WSe_2. Both the <1nm thickness of WSe_2 and compact size of metasurfaces realize a CP controllable ultrathin light source.

2. Experiments

The chiral metasurfaces were fabricated on monolayer WSe_2 to achieve CP emission manipulation as Fig. 1(a) illustrated. We first transferred the chemical vapor deposition (CVD) synthesized monolayer WSe_2 on to a double-side polished fused silica substrate. The metasurfaces were then directly fabricated on WSe_2 through electron beam lithography (EBL) followed by metal deposition (50nm of Au / 3nm of Ti) and lift-off process.

The fabricated chiral metasurfaces were displayed in Fig. 1(b) which composed of plasmonic gold nanorod based chiral metamolecules (CMMs) array. Each CMM contained two identical gold nanorods with 150 nm of length (L), 80 nm of width (W), separated by a 40 nm gap (G) and a lateral shift (S) around L/2. According to the lateral shift direction, the CMMs were divided into two chiral counterparts D_+ and D_- types. These types of CMMs have been reported would behave optical chirality by Meinzer et al. and Cotufo et al. [4,5]

To investigate the WSe_2 CP emission manipulated by the chiral metasurfaces, we first characterize the optical chirality of CMMs themselves through 3D finite element method (3D-FEM) simulation and the CP resolved extinction measurement. The optical chirality manipulating effects on photoluminescence (PL) of WSe_2 was subsequently demonstrated by excited the WSe_2-CMMs hybrid devices under 532 nm continuous-wave laser at 77K. The excitation was modulated as left-handed or right-handed circular polarization (LCP or RCP) and the PL was resolved by a broad-band quarter wave plate and a linear polarizer.

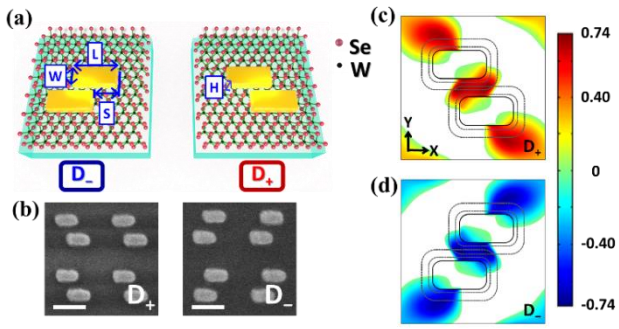

Fig. 1(a) The schematics of chiral metasurfaces on monolayer WSe_2 to manipulate the CP states of emission. (b) Scanning-electron-microscopy images of fabricated SDNRs metasurfaces. The local CD distribution around (c) D_+ and (d) D_- CMMs.

3. Results and Discussion

The nanorod-based design of CMMs provides LSPR along the long axis of each single nanorod and the pair arrangement with a 40 nm gap enable resonant coupling. If the two nanorods are aligned with a finite lateral shift, the reso-

nant coupling occurs in different strength and phase along nanorod long axis. This asymmetric coupling deforms the localized electric field distribution. Furthermore, the electric field vector of CMMs behave a rotary manner with opposite directions between D_+ and D_- CMMs indicated the optical chirality in CMMs structures. The calculated local circular dichroism (CD) distribution around CMMs are expressed as Fig. 1(c) and (d), the CD value is defined as $(I_R-I_L)/(I_R+I_L)$, where I_R and I_L are the RCP and LCP intensities respectively. It can be observed that for D_+ (D_-) type CMMs, the asymmetric coupling resonant mode tend to generate stronger I_R than I_L (I_L than I_R) leading positive (negative) CD. Moreover, the maxima CD is located in the center between two nanorods due to the strongest asymmetric coupling occur.

Fig. 2(a) exhibit the RCP and LCP extinction spectra EXT_R and EXT_L of the D_+ and D_- CMMs, respectively. As LSPR was induced, photons with specific wavelength couple to CMMs and cause significant extinction. The CP component which better matched the polarization of resonant mode in structures trigger the higher extinction peak. The optical chirality of CMMs can be quantified by the CD of extinction as $CD_{EXT}= (EXT_R-EXT_L) / (EXT_R+EXT_L)$. Therefore, we are able to conclude the D_+ (D_-) type CMMs interact with RCP (LCP) light more strongly, generated more substantial EXT_R (EXT_L) peak and obtained positive (negative) CD_{EXT} values as the CD_{EXT} spectra displayed in Fig. 2(b). It should be noted that the maximum $|CD_{EXT}|$ values around 10% are designed at wavelength around 720 nm to match the PL of monolayer WSe_2 under 77K.

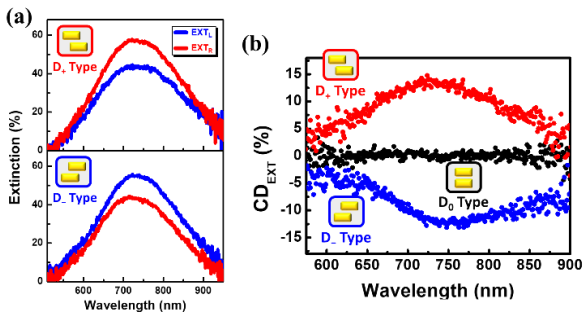

Fig. 2(a) The circularly polarized extinction spectra of (a) chiral D_+ and D_- CMMs. (b) The CD_{EXT} spectra of D_0 / D_+ / D_- CMMs.

To investigate the CP emission of WSe_2 manipulated by CMMs, we first characterized the CP-PL of bare WSe_2 as shown in Fig. 3(a). Due to the valley-selective absorption of WSe_2 at K valley under RCP (LCP) excitation [2], the RCP-PL (LCP-PL) would be slightly stronger. And we could quantify the optical chirality of CP-PL through

$$CD_{PL} = \frac{I_R - I_L}{I_R + I_L} \times 100\% \quad (1)$$

where I_R and I_L are PL intensities resolved in RCP and LCP states. The CD_{PL} of bare WSe_2 under RCP (LCP) was around positive (negative) 6% which are not as high as reported due to the relative high temperature and excitation photon energy far above the bandgap of monolayer WSe_2. However, even in such conditions, we will see the $|CD_{PL}|$ significantly boosted up by the CMMs metasurfaces. Fig. 3(b) shows the CP-PL spectra of WSe_2 integrated with D_- CMMs under LCP excitation which the LCP-PL become much stronger than RCP-PL and bring the CD_{PL} as high as –26.2%. Since the D_- CMMs would couple more photons in the LCP state, and the monolayer WSe_2 also emitted more LCP photons under LCP excitation, the $|CD_{PL}|$ value significantly enhanced to 400% than the CD from bare WSe_2 due to the effect of the addition of these two mechanisms. On the other hand, when the WSe_2 integrated D_+ CMMs under LCP excitation, the $|CD_{PL}|$ magnitude are approximately +20% as displayed in Fig. 2(c) although bare WSe_2 exhibited negative CD_{PL}. It indicated the optical chirality of the RCP-favored D_+ CMMs were robust to reverse the intrinsic CD_{PL} of bare WSe_2.

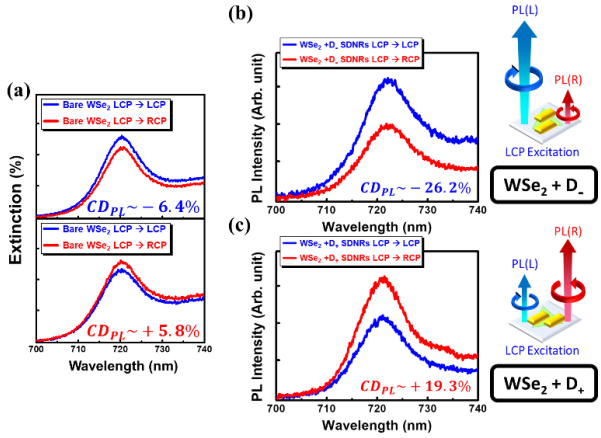

Fig. 3(a) The CP-PL spectra of bare monolayer WSe_2 under RCP and LCP. The CP-PL spectra of WSe_2 integrated with (b) D_- and (c) D_+ SDNRs under LCP excitation. The cartoon at the right of spectra are the schematic of emission CP states.

4. Conclusions

In summary, the CP state controllable ultrathin light source was demonstrated by integrating the plasmonic chiral metasurfaces with WSe_2 atomic layer. The combination of the chiral metasurfaces and chiral emission of monolayer WSe_2 under CP excitation significantly boosted the CD_{PL} to about 400%. Besides, the positive and negative CD_{PL} were both achieved under the same CP state excitation showed the ability to manipulate CP emission. This work provides the platform to apply the TMDC atomic layer in practical applications such chip-scale optical information processing and biosensing.

Acknowledgements

This work was supported by the Innovative Materials and Analysis Technology Exploration Program (IMATE) of Academia Sinica and the Ministry of Science and Technology in Taiwan under the contract number MOST 105-2112-M-001-011-MY3.

References

[1] N. J. Greenfield, Nat. Protoc. **1**, 2876-2890 (2006).
[2] Jones, et al., Nat. Nanotechnol. **8**, 634-638 (2013).
[3] V. K. Valev, et al., Adv. Mater. **25**, 2517-2534 (2013).
[4] M. Cotrufo, et al., ACS Nano **10**, 3389-3397 (2016).
[5] N. Meinzer, et al., Physical Review B **88**, 041407 (2013).